Manaaki Whenua
Landcare Research

Climate change impacts on suspended sediment loads in the Wairoa catchment, Hawke's Bay

Prepared for: Our Land & Water National Science Challenge

June 2022

Climate change impacts on suspended sediment loads in the Wairoa catchment, Hawke's Bay

Contract Report: LC4121

Hugh Smith, Simon Vale, Andrew Neverman, Melissa Robson-Williams, Laise Harris

Manaaki Whenua – Landcare Research

Reviewed by:
Chris Phillips
Senior Researcher
Manaaki Whenua – Landcare Research

Approved for release by:
John Triantafilis
Portfolio Leader – Managing Land & Water
Manaaki Whenua – Landcare Research

Contents

Summary

Project

- The Wairoa River is significant to the iwi and hapū of Te Rohe o Te Wairoa. An important threat to the health of the river is from sediment entering the water.
- The Wairoa Tripartite (Wairoa District Council, Tātau Tātau o Te Wairoa, Hawke's Bay Regional Council) and the Whitiwhiti Ora project (part of the Our Land and Water National Science Challenge) have formed a partnership to jointly guide the direction and delivery of a project focused on understanding cultural values related to the river and the impact of sediment on these values.

Objectives

- The objective of the present report is to model erosion and suspended sediment loads in the Wairoa catchment for baseline and future climate scenarios. This information will inform work assessing sediment impacts on the river's cultural values.

Methods

- Existing SedNetNZ model results for erosion processes were used in combination with an updated algorithm for lake and floodplain sediment storage to estimate mean annual suspended sediment loads for the baseline scenario, represented by recent land cover and climatic conditions.
- The effects of future climate change were modelled for the baseline land cover using rainfall and temperature grids from six regionally downscaled climate models and four climate trajectories at mid- and late century to adjust modelled erosion process rates under climate change and estimate future suspended sediment loads.

Results

- The modelled mean annual suspended sediment load reaching the coast amounts to 2.5 Mt/yr under baseline conditions. Shallow landslide erosion makes the largest contribution to total erosion on average over a multi-decadal timescale.
- Under future climate scenarios, the range in end-of-catchment suspended sediment loads is estimated at 2.8–3.5 Mt/yr and 2.7–4.3 Mt/yr by mid- and late century, respectively. These changes correspond to increases of 10–37% and 7–69% compared to the baseline sediment load by mid- and late century, respectively.

Conclusions

- The modelled climate change projections produce a wide range of predicted changes in suspended sediment load. This reflects the variability between climate models and the diverging climate trajectories.
- Further modelling work is planned within the Whitiwhiti Ora project to examine how different land-use scenarios affect suspended sediment loads under climate change. These scenarios will be developed in partnership with the Wairoa Tripartite.

1 Introduction

The Wairoa River is significant to the iwi and hapū of Te Rohe o Te Wairoa, and is valued ecologically as well as for recreation and mahinga kai. An important threat to the health of the river is from sediment entering the water.

The Wairoa Tripartite (Wairoa District Council, Tātau Tātau o Te Wairoa, Hawke's Bay Regional Council) and the Whitiwhiti Ora project (part of the Our Land and Water National Science Challenge) have formed a partnership to jointly guide the direction and delivery of a project focused on the river, particularly the impact of sediment on this taonga. The Wairoa project aims to:

- understand the values of the local hapū with respect to the river, with a focus on mahinga kai and sites of cultural significance
- assess how sediment affects these values
- inform targeting of sediment sources via intervention scenarios to reduce the impacts of sediment on these values.

In the present report we employ erosion and sediment modelling to quantitatively assess the spatial patterns in erosion across the Wairoa catchment and the suspended sediment loads in the river network. This model-based approach allows us to represent both a contemporary baseline and future climate change scenarios to better understand how climate change might affect the amount of sediment entering the river and reaching the coast. The model can then form the basis for testing the impact of different intervention scenarios and assessing the extent to which such interventions mitigate impacts from climate change.

2 Background

The SedNetNZ sediment budget model was developed to represent the diversity of erosion processes that occur across Aotearoa New Zealand (Dymond et al. 2016; Smith et al. 2019). These comprise shallow landslide, earthflow, gully, streambank, and surficial erosion. The model estimates the average amount of sediment produced by each of these erosion processes per year in the sub-catchment of each stream segment within the digital river network derived for the River Environment Classification (RECv2). The modelled sediment contributions from each erosion process are then routed down the network, accounting for long-term storage of sediment in lakes and on floodplains, to estimate the net mean annual suspended sediment load for every segment in the river network.

SedNetNZ modelling was previously undertaken for the Wairoa catchment as part of an application of the model to northern Hawke's Bay (Spiekermann et al. 2017). This work was completed for Hawke's Bay Regional Council (HBRC) alongside SedNetNZ applications for the Tukituki River catchment (Palmer et al. 2017) and the Tūtaekurī, Ahuriri, Ngaruroro, and Karamu catchments (together referred to as TANK), along with the South Coast and Pōrangahau catchments (Palmer et al. 2016), to provide complete model coverage for the

region. These studies showed that, on average, shallow landslide erosion made the largest contribution to predicted suspended sediment loads, with further significant contributions from surficial and bank erosion sources. The importance of shallow landslide erosion as a sediment source is consistent with findings from post-storm erosion mapping and analysis of lake sediment records in the region (Page et al 1994; Trustrum et al. 1999).

Subsequently, the streambank erosion component of SedNetNZ was updated for the whole region at the request of HBRC (Smith et al. 2020). This update replaced the previous estimate of suspended sediment loads from bank erosion with estimates based on an improved bank erosion model described in Smith et al. 2019. While this mostly resulted in a minor change in modelled sediment loads, it provided an improved basis for representing spatial patterns in bank erosion by including a range of factors that influence bank erosion at the scale of individual segments in the river network (Smith et al. 2020).

Since the completion of modelling in the Wairoa catchment and across the wider Hawke's Bay region, SedNetNZ has undergone several updates. These include the representation of lake sediment trapping as part of a revised river network routing algorithm (Neverman et al. 2022), while the floodplain deposition algorithm has been refined to better represent spatial patterns in floodplain deposition based on upstream loads delivered to each stream segment rather than averaging the load deposited on floodplains across major catchments (Vale et al. 2021).

In the present report we describe an approach for combining SedNetNZ with projected changes in climate to estimate potential impacts on suspended sediment loads in the Wairoa catchment by mid- and late century. We use the previous SedNetNZ estimates of erosion process contributions to suspended sediment loads, including the updated bank erosion loads, to represent recent land cover and climate conditions. We then apply the revised algorithm representing lake and floodplain sediment storage to estimate the net mean annual suspended sediment load in the river network under recent conditions. This replaces the previous estimates of floodplain deposition and suspended sediment loads for the Wairoa catchment reported by Spiekermann et al. (2017) and Smith et al. (2020). These updated suspended sediment loads form a baseline for comparison with predictions of loads under future climate change.

3 Wairoa catchment description

The Wairoa catchment covers an area of 3,674 km^2 and drains the eastern flanks of the Huiarau Range (Figure 1). It is characterised by hill country and hilly steeplands underlain by soft sedimentary rocks, including mudstones and sandstones, with extensive areas of tephra (Figure 2). Land cover is predominantly pasture, but indigenous forest occurs across the mountain ranges and there are areas of exotic forest in the hill country (Figure 3). The catchment is highly erosion prone, with extensive shallow landslide erosion occurring in response to high-magnitude rainfall events (Douglas et al. 1986). Gully and earthflow erosion processes also occur in some areas (Figure 2).

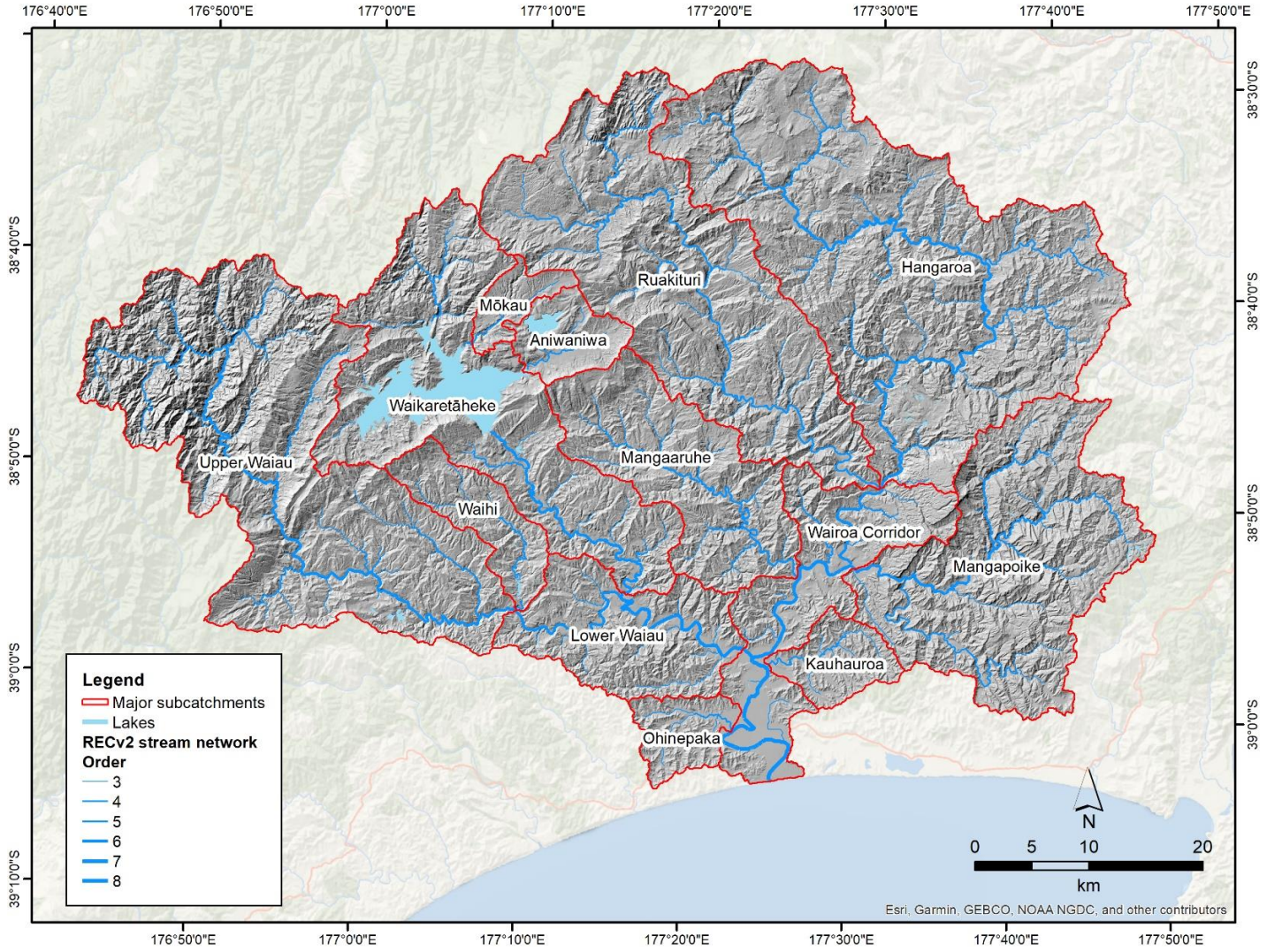

Figure 1. River network of the Wairoa catchment based on RECv2 with major sub-catchment boundaries and names, and hill shade relief based on a 15 m digital elevation model (DEM). Sub-catchment names and boundaries are based on HBRC's Water Management Catchments layer.

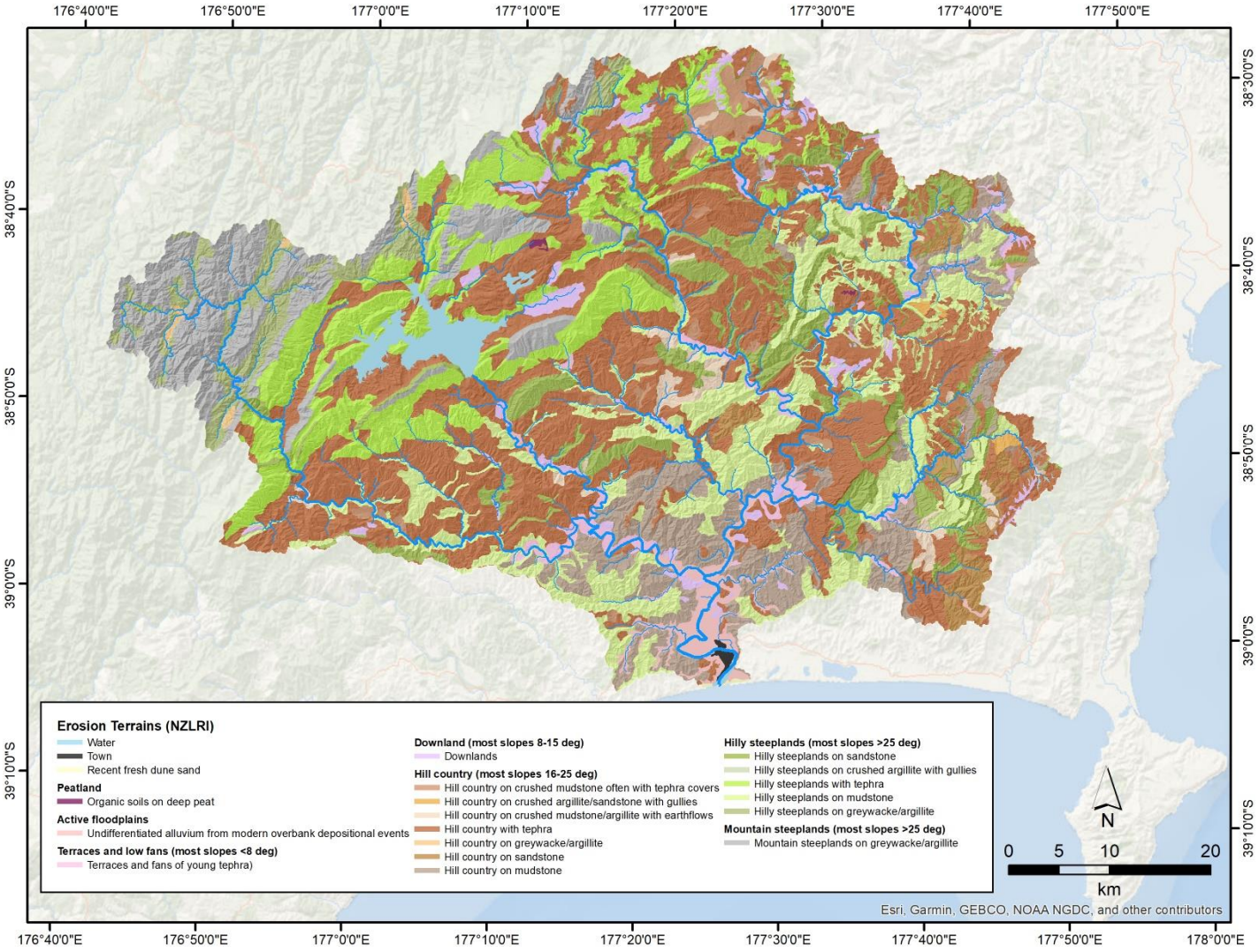

Figure 2. Erosion terrains of the Wairoa catchment. The erosion terrains are used in the SedNetNZ model and based on the 1:50,000 NZ Land Resource Inventory (NZLRI).

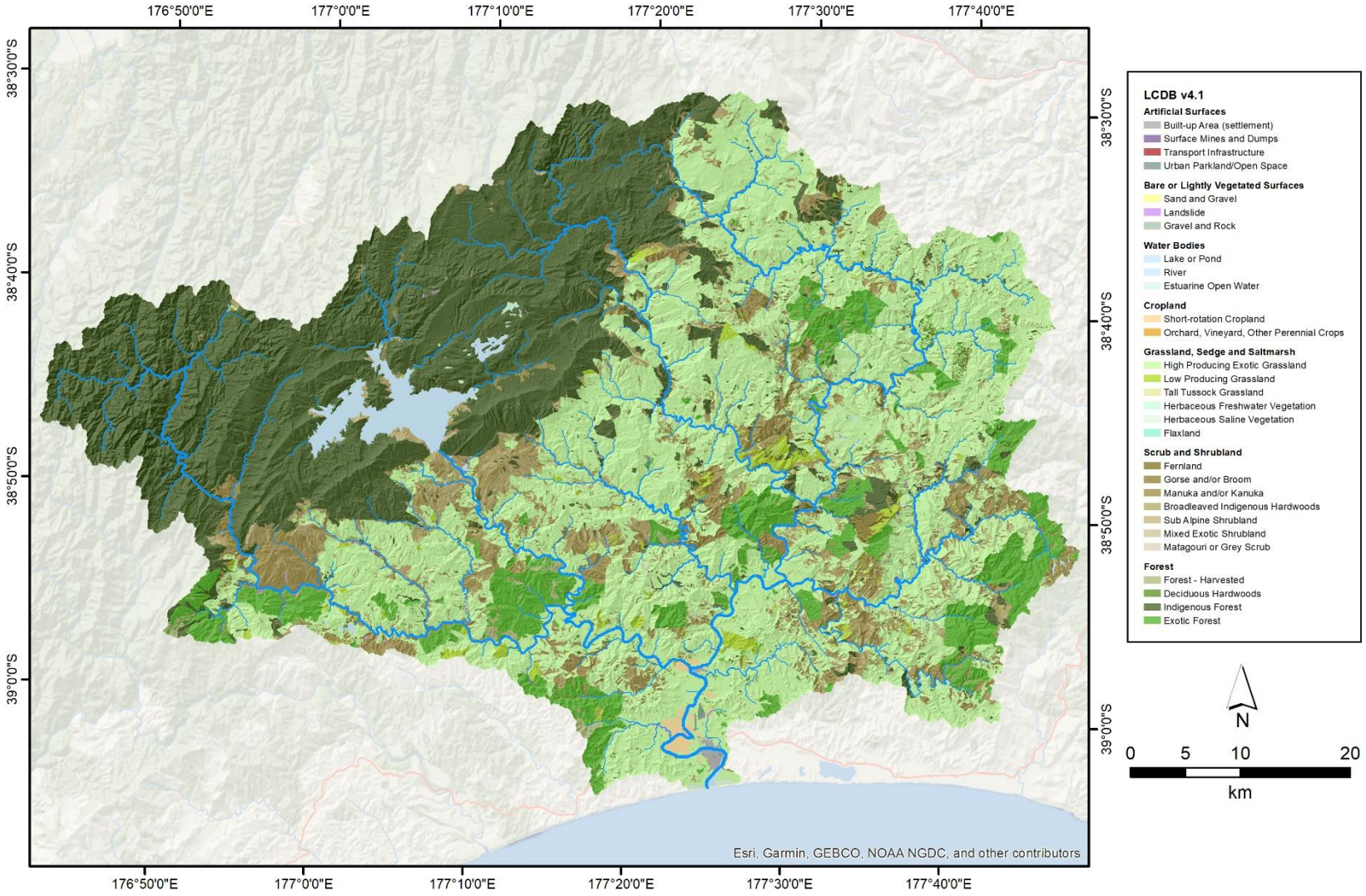

Figure 3. Land cover and tributaries of the Wairoa catchment. Land cover used in both the previous SedNetNZ modelling and the present study is based on the Land Cover Database (LCDB v4.1) for consistency.

4 Methods

4.1 SedNetNZ model description

The following section describes the erosion processes represented in SedNetNZ. The descriptions of surficial, shallow landslide, earthflow, and gully erosion are based on Spiekermann et al. 2017, while the updated bank erosion component of the model is summarised from Smith et al. 2020. The section also outlines the revised river network routing algorithm, which incorporates lake and floodplain sediment storage.

4.1.1 Surficial erosion

Surficial erosion processes in SedNetNZ (Dymond et al. 2016) are represented by the New Zealand Universal Soil Loss Equation (NZUSLE; Dymond et al. 2010) model:

$$ES = a\,P^2\,K\,(\frac{L}{22})^{0.5}\,F_s\,C \quad (1)$$

where ES denotes surficial erosion in t/km^2/yr, a is a constant (t/km^2/yr/mm^2); P is mean annual rainfall (mm); K is a soil erodibility factor (0.25 for loam soil, based on Dymond et al. 2010; L is slope length (m); F_s is a slope steepness factor, given by $0.065 + 4.56\,\mathrm{s} + 65.41\,\mathrm{s}^2$, where s is slope gradient; and C is a vegetation cover factor (1.0 for bare ground, 0.01 for pasture, 0.005 for forest, dimensionless).

4.1.2 Shallow landslide erosion

Shallow landslides are considered the most common form of erosion in New Zealand hill country (Eyles 1983). Typical landslides are seldom greater than 2 m deep, and individual failures are usually of small areal extent (50–100 m^2) (Smith et al. 2021). Landslides generally have a tail of deposited sediment below their source that often reaches a stream (for approximately half of debris deposits; see Dymond et al. 1999). Landslide occurrence is highly correlated with slope angle, with most failures occurring on slopes steeper than 26 degrees, but landslides can occur on slopes as low as 15 degrees (De Rose 2013; Smith et al. 2021).

Landslide erosion is estimated for those erosion terrains (Figure 2) identified as susceptible to landslide erosion. An erosion terrain is a land type with a unique combination of erosion processes and rates leading to characteristic sediment generation and yields. Erosion terrains were derived from New Zealand Land Resource Inventory data and are based on combinations of rock type, topography, rainfall, and erosion process type and severity. Erosion terrain classes are listed in Dymond et al. 2010.

The expected mass of soil lost to landslide erosion per square kilometre per year, and the connection with a stream, is given by EL:

$$EL = \rho\,SDR\,d_l f(s) \quad (2)$$

where ρ is the bulk density of soil (t/m^3), SDR is the sediment delivery ratio, d_l is the mean depth of landslide failure (m), and $f(s)$ is the expected area of landslide scars per square

kilometre per year at slope angle s (m^2/km^2/yr). ρ is set to 1.5 t/m^3 (Dymond et al. 2016); *SDR* is set to 0.5 for hill country and 0.1 for mountain terrain (Dymond et al. 2016); d_l is set to 1 m (Page et al. 1994; Reid & Page 2003); and *f(s)* was determined from previous analysis of historical aerial photographs, where the average proportion of eroded bare ground is determined for different slope classes (Dymond et al. 2016; Betts et al. 2017).

4.1.3 Earthflow erosion

Slow-moving earthflows are common in erosion terrains underlain by crushed mudstone and argillite (Dymond et al. 2010). The delivery of sediment to streams is via the undercutting of earthflow toes. The mass of soil delivered to streams by earthflows in t/km^2/yr is denoted by EE and is estimated as:

$$EE = \rho\, d_e\, v\, ED \quad (3)$$

where ρ is the bulk density of soil (t/m^3), d_e is the mean depth of earthflows (m), v is the mean speed of earthflows (m/yr), and ED is the mean length of stream intersecting earthflow toes in a square kilometre (m/km^2).

ρ is set to 1.5 t/m^3 (Dymond et al. 2016), d_e is set to 3 m (based on field observation; Dymond et al. 2016), and v is set to 0.1 m/yr (average from published data; Guy 1977; Zhang et al. 1991; Marden et al. 2008, 2014). ED is set to 1,024 m/km^2 (from digitising stream lengths on scanned aerial photographs; Dymond et al. 2016).

4.1.4 Gully erosion

Gullies commonly initiate at channel heads, usually because of excessive surface or subsurface water flow. Once initiated, a gully can continue to expand over long time periods (decades). The mass of soil delivered to streams by gullies, in t/km^2/yr, is denoted by EG and is estimated by:

$$EG = \frac{\rho\, A_g\, GD}{T} \quad (4)$$

where ρ is the bulk density of soil (t/m^3), A_g is the mean cross-sectional area of gullies (m^2), GD is the length of gullies in a square kilometre (km/km^2), and T is the estimated time since gully initiation (yr). Following Dymond et al. 2016, ρ is set to 1.5 t/m^3, A_g is set to 900 m^2 (from field observations), GD is set to 220 m (from digitising gully lengths on scanned aerial photographs), and T is 100 years.

4.1.5 Bank erosion

The mass of material eroded from riverbanks each year is a function of bank height, reach length, and bank migration rate:

$$B_j = \rho M_j H_j L_j \quad (5)$$

where B_j is the total eroded mass for the jth stream segment (t/yr), ρ is the bulk density of the bank material (t/m^3), M_j is the bank migration rate (m/yr), H_j is the mean bank

height (m), and L_j is the length (m) of the jth stream segment. Bank height is derived from a relationship with mean annual discharge (Dymond et al. 2016). Bulk density is estimated at 1.5 t/m^3.

The predicted mass of material eroded from riverbanks represents the gross contribution of sediment supplied to the river channel per year. This does not account for redeposition and storage of eroded bank material on banks or within the channel bed, or the lateral accretion of material on bars with channel migration. Hence, net bank erosion in SedNetNZ is estimated as one-fifth of gross bank erosion based on results from the Waipaoa River catchment (De Rose & Basher 2011). Overbank vertical accretion of fine sediment on floodplains beyond the active channel is represented separately (Dymond et al. 2016).

Bank migration rate (M_j) is represented as a function of six factors, as follows:

$$M_j = SP_j Sn_j T_j V_j \left(1 - PR_j\right)\left(1 - PW_j\right) \quad (6)$$

where M_j is the bank migration rate (m/yr) of the jth stream segment, SP_j is the stream power of the mean annual flood (MAF_j) for the jth stream segment, Sn_j is the channel sinuosity rate factor of the jth segment, T_j is the soil texture-based erodibility factor of the jth segment, V_j is the valley confinement factor of the jth segment, PR_j is the proportion of riparian woody vegetation of the jth segment, and PW_j is the fraction of bank protection works for the jth segment (Smith et al. 2019).

SP_j of the MAF_j (m^3/s) is estimated for each stream segment by the product of MAF_j and channel slope (S_j). MAF_j is estimated from a fitted power relationship ($MAF = 39q^{0.8}$, R^2 = 0.84) with mean annual discharge (q, m^3/s) using data from 26 gauging stations across Hawke's Bay (Smith et al. 2020):

$$SP_j = MAF_j S_j = 39{q_j}^{0.8} S_j \quad (7)$$

Mean annual discharge estimated for each segment in the RECv2 digital river network is based on an empirical water balance model (Woods et al. 2006) used in the CLUES water quality model (Elliott et al. 2016).

We use the log-normal probability density function to represent the relationship between channel sinuosity and migration rate, which we term the sinuosity rate factor. This function allows us to represent the positive skew observed in the relationship between channel sinuosity and migration rate (Crosato 2009). The dimensionless channel sinuosity rate factor (Sn_j) is calculated as

$$Sn_j = \frac{1}{(Sinu_j - 1)\sigma\sqrt{2\pi}}\, e^{\left(-\frac{\left(\ln\left(Sinu_j - 1\right) - \mu\right)^2}{2\sigma^2}\right)} \quad (8)$$

where $Sinu_j$ is sinuosity of the jth stream segment of the RECv2 network, and μ and σ are the mean and standard deviation parameters that determine the location and scale of the distribution. The μ and σ parameters are fitted using bank migration rate data.

The texture of bank material influences bank migration rates (Hickin & Nanson 1984; Julian & Torres 2006; Wynn & Mostaghimi 2006). Our approach is based on an empirical relationship between percentage silt + clay content (SC) and soil critical shear stress (τ_c) derived by Julian and Torres (2006) using data from Dunn (1959) as follows:

$$\tau_c = 0.1 + 0.1779SC + 0.0028SC^2 - 0.0000234SC^3 \quad (9)$$

SC is obtained from spatial data on soil textural classes compiled from the Fundamental Soil Layers (FSL) (Newsome et al. 2008), which provide national coverage. The soil texture-based erodibility factor (T_j) is represented by a power function to characterise the relationship between τ_c and bank erodibility for the jth stream segment:

$$T_j = c{\tau_{c,j}}^{-d} \quad (10)$$

where the c and d parameters are fitted using bank migration rate data. The choice of a power function is based on experimental (Arulanandan et al. 1980) and field (Hanson & Simon 2001; Julian & Torres 2006) observations of the relationship between stream bank or bed critical shear stress and erodibility.

Floodplain extent and the level of valley confinement are factors that may limit lateral bank migration (Hall et al. 2007; De Rose & Basher 2011). The presence of steep valley sides and/or exposure of bedrock influence spatial patterns of erosion and deposition (Fryirs et al. 2016). We estimate a valley confinement factor (V_j) by using the mean slope (SB_j) in degrees of a buffer zone either side of the jth stream segment:

$$V_j = \left(1 - e^{\left(-15/SB_j\right)}\right)^{11} \quad (11)$$

Woody riparian vegetation typically increases bank stability via the effects of (a) root reinforcement and root cohesion (Abernethy & Rutherfurd 2000; Hubble et al. 2010; Polvi et al. 2014; Konsoer et al. 2016), (b) increased flow resistance (Thorne 1990), and (c) lowering bank water content through canopy interception and evapotranspiration (Simon & Collison 2002). We represent the effect of riparian woody vegetation (PR_j) in reducing bank migration rates at the reach scale. Bank migration rates are reduced proportionally to the extent of woody riparian vegetation along the j^{th} stream segment (equation 6). Stream segments with complete riparian woody vegetation cover are assumed to erode at 0.05 of the migration rate for segments with no woody cover (De Rose et al. 2003).

Spatial information on woody vegetation was obtained from satellite imagery and intersected with the Land Information New Zealand (LINZ) digital stream network obtained from 1:50,000 topographic mapping. The mapped stream network was used in preference to the national DEM-derived channel network because it tends to exhibit better planform accuracy, which improves spatial correspondence between channel position and riparian woody vegetation. The proportion of riparian woody vegetation is computed from the intersection of the LINZ stream network with a 15 m buffer and a classified map of woody vegetation cover, which was derived from Landsat TM at 15 m resolution (Dymond & Shepherd 2004).

We also include representation of channel protection works (PW_j) that are designed to reduce bank erosion (e.g. rock riprap, willow edge protection) as well as stopbanks employed for flood protection, where such data are available. We assume that over the multi-decadal model timescale, erosion mitigation would ultimately be targeted to where migrating riverbanks approach stopbanks, or that such interventions have already been implemented to protect stopbank integrity. The proportional length of channel erosion protection measures and stopbanks is summed to give the proportion of channel works (PW_j) for the jth stream segment.

4.1.6 Sediment deposition and river network routing

SedNetNZ accounts for the deposition of sediment in lakes and on floodplains as the sediment is transported through the river network. The description provided here relates to model developments that occurred following applications to the Wairoa catchment and the wider Hawke's Bay region, and thus differ from the description in Spiekermann et al 2017.

To estimate the quantity of sediment trapped in lakes, we apply a revised SedNetNZ sediment routing algorithm (Neverman et al. 2022). The revised routing algorithm applies a lake-specific sediment passing factor (SPF) to the routed sediment load at the end of a RECv2 sub-catchment draining to a lake. SPF was calculated using an adaptation of Gill's (1979) approximation of Brune's (1953) trap efficiency (the inverse of passing factor) curve for medium sediment:

$$SPF = 1 - \frac{{}^{V}/_{I}}{1.02({}^{V}/_{I})+0.012} \quad (12)$$

where V is the lake volume and I is the annual inflow to the lake.

We also apply an updated algorithm to represent floodplain deposition (Vale et al. 2021). The mass of sediment deposited on the floodplain for a stream segment sub-catchment containing an area of floodplain is calculated as:

$$F_i = pS_t \frac{L_i accS_i{}^2}{\sum L_i accS_i{}^2} \quad (13)$$

where $F_i$is the total floodplain deposition (t/yr) in the ith sub-catchment; p is the proportion of the sediment load generated by hillslope erosion per lake or sea-draining catchment that is deposited on floodplains in the catchment, set to 5% based on previous SedNetNZ parameterisation (Dymond et al. 2016); S_t is the total sediment load (t/yr) generated by hillslope erosion per lake or sea-draining catchment; L_i is the reach length (m) on floodplain in the ith sub-catchment; and $accS_i$ is the total accumulated (upstream) sediment from hillslope erosion (t/yr) in the ith sub-catchment.

4.2 Climate change impacts on erosion processes and sediment loads

The effects of future climate change on erosion and suspended sediment loads are modelled following the approach of Basher et al. (2020). Six CMIP5 (Coupled Model Inter-comparison Project) global climate models (GCMs) (BCC-CSM1.1, CESM1-CAM5, GFDL-

CM3, GISS-E2-R, HadGEM2-ES, and NorESM1-M) were coupled with the New Zealand Regional Climate Model (Sood 2014) by the Ministry for the Environment (2018) to characterise future temperature and precipitation to 2100 on a 5 km grid. These GCMs were chosen based on their performance assessed against historical climate and representation of the likely range in model sensitivity (Collins et al. 2018; Ministry for the Environment 2018).

Four forcing scenarios from the Intergovernmental Panel on Climate Change Fifth Assessment Report (IPCC AR5) (IPCC 2013), known as representative concentration pathways (RCPs), are used to drive the models, and represent different radiative forcing based on greenhouse gas trajectories (Table 1; Ministry for the Environment 2018). The RCP pathways represent total radiative forcing of 2.6 W/m^2 (a mitigation pathway), 4.5 W/m^2 and 6.0 W/m^2 (stabilisation pathways), and 8.5 W/m^2 (very high greenhouse gas concentrations), referred to as RCP2.6, RCP4.5, RCP6.0, and RCP8.5, respectively. Differences in the climate change scenarios (RCPs) become more evident after 2035 due to divergence in the radiative forcing pathways (Figure 4).

The effects of climate change on erosion processes are represented in SedNetNZ using different climatic variables to drive changes in different erosion processes. In the hillslope domain, surficial erosion is modelled for each climate scenario using the estimated change in mean annual rainfall from the regional climate models (RCMs) to directly adjust P in equation 1 (Basher et al. 2020). Mass movement erosion is assumed to change as a function of changing storminess (i.e. a change in storm total rainfall resulting from changes in the frequency and magnitude of storm events) across the region. This change in storminess is used to derive a proportional change in the density of shallow landslides that occur under each climate scenario, which is used to represent a change factor, CF, in all hillslope mass movement-dominated erosion processes, following Manderson et al. (2015), Basher et al. (2020), and Neverman, Donovan et al. (2021).

Table 1. Representative concentration pathway scenarios and their descriptions

Representative concentration pathway (RCP)	Description
2.6	Mitigation scenario, requiring removal of CO_2 from the atmosphere
4.5	Intermediate scenario where CO_2 concentrations stabilise
6.0	Intermediate scenario where CO_2 concentrations stabilise
8.5	Continual increase in CO_2 concentrations (representing a worst-case scenario)

Source: Ministry for the Environment 2018

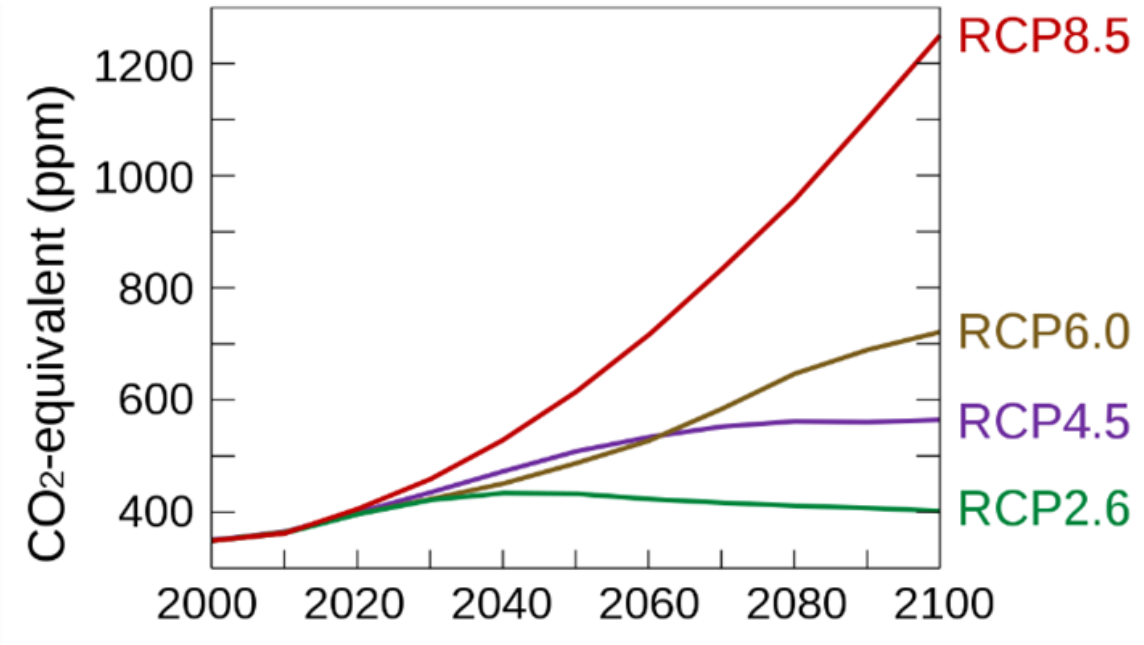

Figure 4. CO_2-equivalent concentration pathways, referred to as representative concentration pathways (RCPs), based on the IPCC Fifth Assessment Report.

The change in storminess under each climate scenario is calculated by adjusting historical rainfall records (CliFlo; NIWA 2021) by an augmentation factor based on predicted changes in storm rainfall resulting from the change in temperature related to increased CO_2-equivalent concentrations:

$$R' = R(1 + \Delta T\ AF) \tag{14}$$

where R' is future rainfall, R is historical rainfall, ΔT is future absolute change in temperature relative to baseline, and AF is the augmentation factor. AF is derived from the estimated change in rainfall depth per 1°C increase in temperature calculated by the Ministry for the Environment (2018) for a 48-hour duration rainfall event with an average recurrence interval of 30 years, which is assumed to represent the dominant landslide triggering event (Basher et al. 2020), giving a value of 0.073. Rain gauges with complete records for the last 50 years were selected from CliFlo (NIWA 2021) and used to represent historical daily rainfall. At each gauge, equation 14 was used to calculate R' under temperature changes up to 3°C.

Storm events were then identified in the baseline and future rainfall records as consecutive days where rainfall exceeded 10 mm per day. The storms were considered landslide-producing events if >150 mm of rain fell in a 48-hour period during the event. The total rainfall for the storm event was used to estimate the density of shallow landslides produced in each rainfall record for baseline and climate scenarios using the relationship between storm total rainfall and shallow landslide density identified by Reid and Page (2003):

$$LD = mR_s + b \tag{15}$$

where LD is the density of shallow landslides per km^2; R_S is the total rainfall for the storm event; m is the slope of the linear relationship between LD and R_s and was set to 0.72

(Basher et al. 2020); and b is the y-intercept of the relationship, calculated by solving for b under the assumption LD = 0 when $R_s \leq$ 150 mm:

$$0 = 150m + b \tag{16}$$

$$b = -136.8 \tag{17}$$

Linear models were developed for the relationship between LD and ΔT at each rain gauge location, and can be used to estimate the future landslide density given a change in temperature:

$$LD' = a\Delta T + LD \tag{18}$$

where LD' is the future landslide density; a is the slope of the linear relationship between ΔT and LD', and therefore the absolute change in landslide density per 1°C of temperature change; and LD is the landslide density for the baseline rainfall record, R.

The change factor, CF, is then calculated at each rain gauge as the proportional increase in landslide density per 1°C of temperature change, calculated as:

$$CF = \frac{a}{LD} \tag{19}$$

CF was then interpolated spatially using Sibson's (1981) natural neighbours interpolation based on the selected rain gauges, which included eight from the Hawke's Bay region and four from Gisborne. No gauges were available for selection from within the Wairoa catchment.

Future rates of mass movement, MM', are then calculated by augmenting the baseline mass movement rate, MM, by CF and the change in temperature, ΔT, at the i^{th} pixel of the 5 km temperature change grids for each climate scenario, such that:

$$MM' = MM(1 + CF\Delta T_i) \tag{20}$$

where MM represents the hillslope mass movement-dominated processes, EL, EE, and EG, from equations 2 to 4.

The effect of climate change on bank erosion is based on estimated changes in MAF_j for each climate scenario, per stream segment. MAF has been previously used as a spatial predictor of streambank erosion (Dymond et al. 2016; Smith et al. 2019). Future changes in MAF were estimated based on hydrological modelling that simulated flows over successive 20-year periods for each RCM and RCP (Collins et al. 2018) and computed proportional changes in future MAF relative to a historical baseline period (1986–2005). These predicted proportional changes in future MAF were available as the median across the six RCMs for each RCP but not for individual RCMs (Neverman, Donovan et al. 2021). We therefore use these median values with each RCM.

Future net suspended sediment loads from bank erosion (t/yr) for the jth stream segment under climate change (B_j') were estimated as

$$B_j' = B_j \Delta MAF_j \tag{21}$$

where B_j is the baseline net suspended sediment load from bank erosion (equation 5) and ΔMAF_j is a dimensionless change factor based on the change in MAF between the baseline and future climate scenarios.

Future mean annual suspended sediment loads estimated from climate-driven changes in surficial, mass movement, and bank erosion processes in the Wairoa catchment are computed for mid-century (2031–2050, represented by 2040) and end-of-century (2080–2100, represented by 2090) for each RCP. Percentage changes in future suspended sediment loads are relative to the modelled baseline mean annual suspended sediment load for each segment in the digital river network. Climate change effects are reported for each RCP based on the upper, lower, and median projected changes in erosion across the six RCMs at mid- and late century.

5 Results

5.1 Baseline suspended sediment loads

The modelled mean annual suspended sediment load for the Wairoa catchment reaching the coast amounts to 2.5 Mt/yr under baseline climatic and land-cover conditions. This load is slightly lower than the value of 2.7 Mt/yr reported in Smith et al. 2020 following the update to the bank erosion component of SedNetNZ for HBRC. This small reduction in modelled load reflects the inclusion of lake sediment trapping in the present model application.

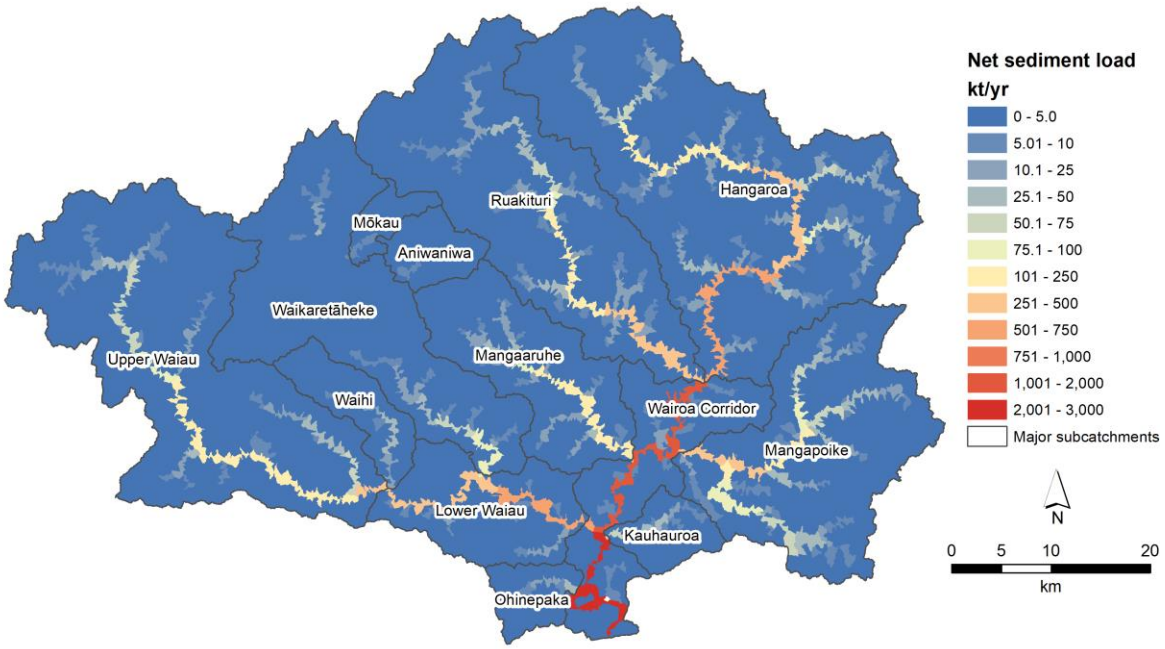

Figure 5. Modelled baseline mean annual net suspended sediment load (kt/yr) for each RECv2 sub-catchment across the Wairoa catchment, with the boundaries of major tributary sub-catchments shown. Net sediment load accounts for lake sediment trapping and floodplain deposition.

Major sub-catchment suspended sediment loads include 0.70, 0.60, and 0.41 Mt/yr from the Hangaroa, Waiau, and Mangapoike tributaries, respectively. Mean annual suspended sediment loads are shown with major sub-catchment boundaries in Figure 5. These are net suspended sediment loads that accumulate downstream while accounting for losses of sediment into long-term storage in lakes and on floodplains.

Suspended sediment load can be expressed as a sediment yield per RECv2 sub-catchment. The Wairoa catchment contains 9,516 RECv2 sub-catchments with an average sub-catchment area of 0.39 km^2. The sediment yield is calculated as the sum of sediment loads from all erosion processes present within each RECv2 sub-catchment divided by the sub-catchment area. This does not account for downstream storage of sediment in lakes and on floodplains.

Figure 6 shows the spatial pattern in mean annual suspended sediment yield ($t/km^2/yr$) for each RECv2 sub-catchment. The largest sediment yields typically occur in areas of pastoral hill country on erodible, soft-rock terrain (Figure 2) as well as along sections of eroding river channel. Lower sediment yields occur in areas with woody vegetation cover or low slope (Figure 3). In a few cases, high yields ($t/km^2/yr$) occur in sub-catchments despite having relatively low erosion (t/yr) due to their very small areas (<0.05 km^2).

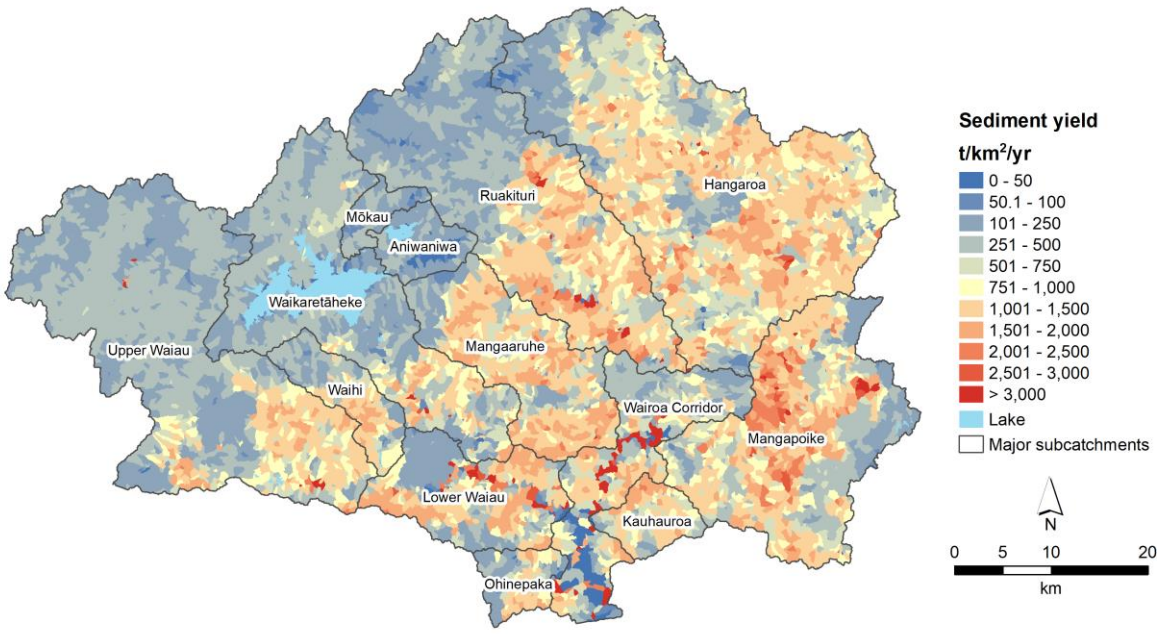

Figure 6. Modelled baseline suspended sediment yield ($t/km^2/yr$) for each RECv2 sub-catchment in the Wairoa catchment.

Shallow landslide erosion makes the largest contribution to total erosion on average over a multi-decadal timescale (Figure 7). Total erosion refers to the sum of sediment loads from all erosion processes and does not account for losses of sediment to storage in lakes or on floodplains. For the whole Wairoa catchment, shallow landslide erosion contributes 71% of total erosion, while surficial (19%) and bank (8%) erosion are the next largest

contributors, followed by earthflow (1.4%) and gully (0.6%) erosion. Among the major sub-catchments, the estimated long-term average contribution of landslides to total erosion varies between 38 and 90%, while surficial erosion ranges between 7 and 62%.

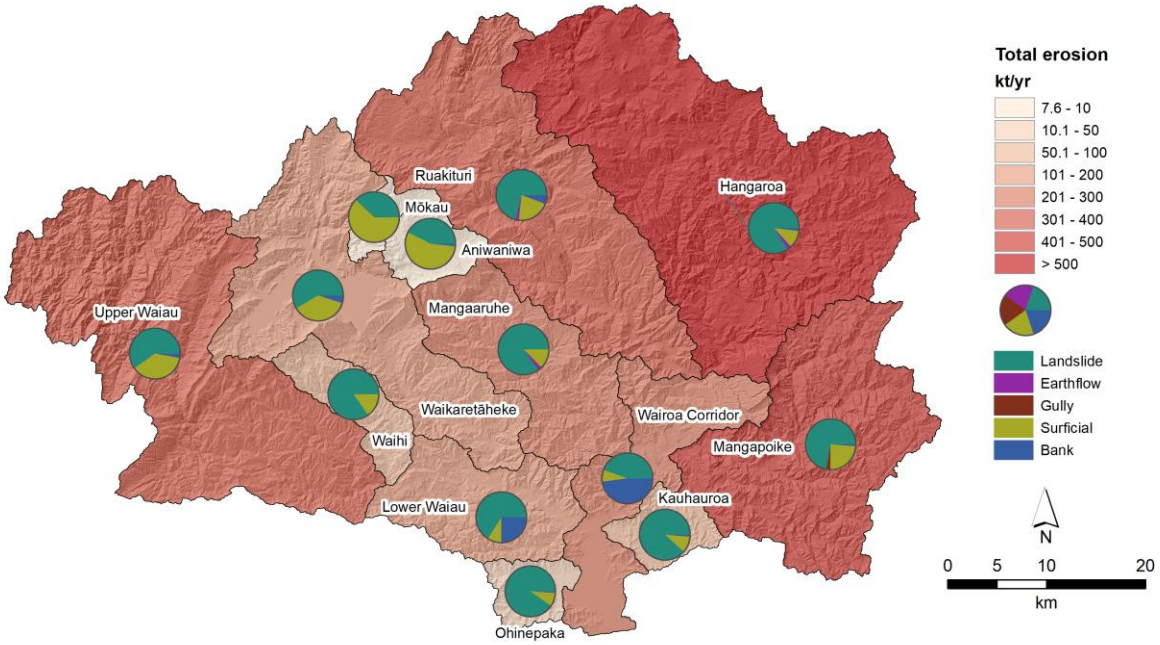

Figure 7. Modelled baseline total erosion (kt/yr) and erosion process load contributions for major sub-catchments in the Wairoa catchment. Total erosion represents the sum of sediment loads from all erosion processes and does not account for losses of sediment to storage in lakes or on floodplains.

5.2 Climate change impacts on suspended sediment loads

The modelled climate change projections produce a wide range of predicted changes in suspended sediment loads. This reflects the variability between climate models and the diverging climate trajectories represented by each RCP (Figure 4).

RCP2.6 represents a mitigation pathway resulting in the lowest sediment load increases, with late-century loads lower than mid-century in many cases (Tables 2 and 3). RCP4.5 and RCP6.0 are stabilisation pathways, and RCP8.5 represents a pathway with very high greenhouse gas concentrations that results in the largest projected increases in sediment load (Tables 2 and 3). Therefore, suspended sediment loads are expected to increase from RCP2.6 to RCP8.5 at mid- and late century, with more pronounced differences between each RCP observed at late century relative to the mid-century projections.

For the Wairoa catchment, the mean annual suspended sediment load delivered to the coast is projected to increase from the baseline 2.5 Mt/yr to 2.8–3.5 Mt/yr and 2.7–4.3 Mt/yr by mid- and late century, respectively, across the range of RCPs. These changes correspond to increases of 10–37% (Table 2) and 7–69% (Table 3) compared to the

baseline sediment load by mid- and late century, respectively. A smaller increase in load is projected by late century (median 11%) compared to mid-century (median 14%) under the mitigation pathway represented by RCP2.6.

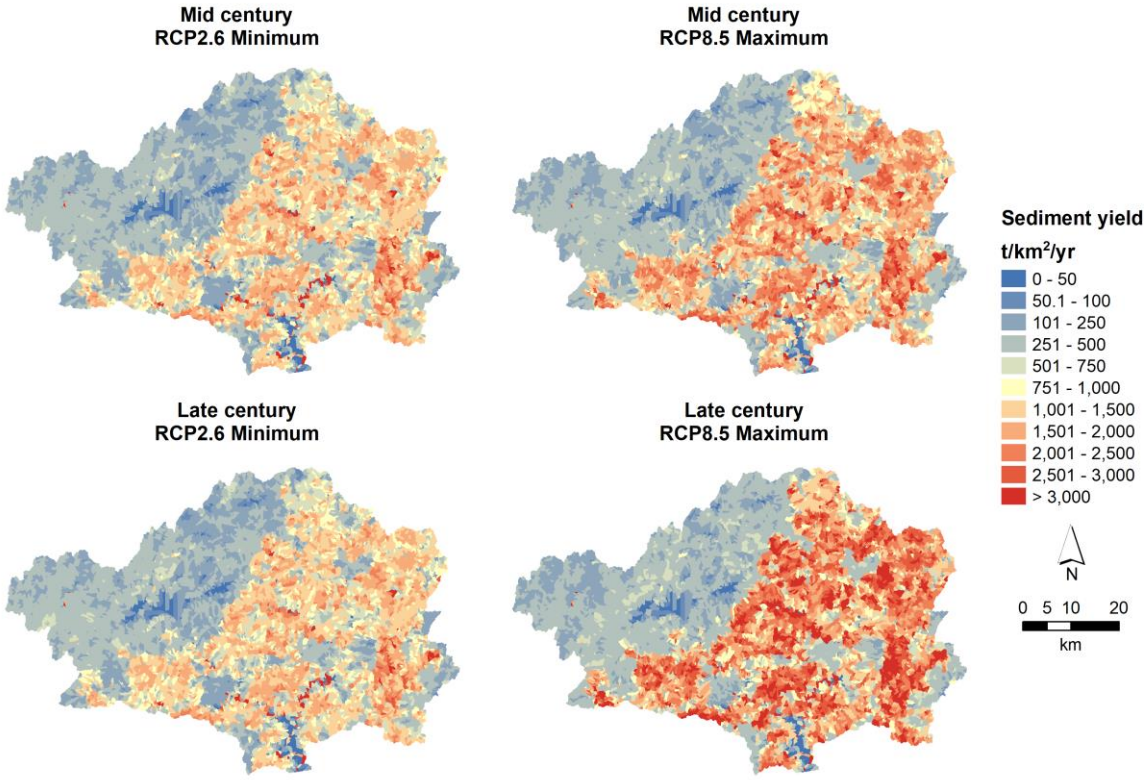

Figure 8. Modelled suspended sediment yield (t/km^2/yr) for each RECv2 sub-catchment for selected climate change scenarios across the Wairoa catchment.

Figure 8 shows the difference between the lower and upper projected increases in sediment yields by comparing RCP2.6 (minimum) versus RCP8.5 (maximum) at mid- and late century. This figure spatially highlights the contrast between the minor decrease in yields for RCP2.6 versus the substantial increase for RCP8.5 between mid- and late century.

For major sub-catchments there is considerable variation in the projected increase in sediment load at mid- (Table 2) and late (Table 3) century across the RCPs. Sediment loads from the Aniwaniwa and Mōkau sub-catchments are the least affected by climate change, with increases ranging from 6 to 20% and 5 to 33% at mid- and late century, respectively. By contrast, the largest increases in sediment load occur in the Hangaroa, Kauhauroa, Mangaaruhe, Ohinepaka, and Waihi sub-catchments, where increases span 12–48% and 8–86% at mid- and late century, respectively. The comparative resilience of Aniwaniwa and Mōkau reflects, in part, the fact that these two sub-catchments are largely forested, which mitigates the impact of increased storminess under climate change, resulting in a smaller increase in landslide erosion compared to the predominantly pastoral hill country sub-catchments.

Climate change projections indicate a trend of decreasing average annual rainfall across the Wairoa catchment towards late century, while the size and frequency of high-magnitude but infrequent storm events is projected to increase. As a result, surficial erosion may tend to decrease on average due to generally lower annual rainfall, while landslide erosion may increase due to the more frequent occurrence of large storm events that trigger a landslide response. The projected magnitude of increase in landslide erosion over the longer term generally exceeds the potential decrease in surficial erosion, resulting in a net increase in modelled mean annual suspended sediment loads across the major sub-catchments and for the whole catchment.

Table 2. Net suspended sediment loads for the whole Wairoa catchment and major sub-catchments under baseline conditions and projected climate change at mid-century. 'Diff' refers to the percentage difference between the sediment load under climate change compared to the baseline load.

Time period	RCP	Selected RCMs[1]	Wairoa catchment[2]		Aniwaniwa[3]		Hangaroa		Kauhauroa		Mangaaruhe		Mangapoike		Mōkau[3]		Ohinepaka		Ruakituri		Upper Waiau		Waiau[4]		Waihi		Waikaretāheke	
			Load (kt/yr)	Diff (%)	Load (kt/yr)	Diff (%)	Load (kt/yr)	Diff (%)	Load (kt/yr)	Diff (%)	Load (kt/yr)	Diff (%)	Load (kt/yr)	Diff (%)	Load (kt/yr)	Diff (%)	Load (kt/yr)	Diff (%)	Load (kt/yr)	Diff (%)	Load (kt/yr)	Diff (%)	Load (kt/yr)	Diff (%)	Load (kt/yr)	Diff (%)	Load (kt/yr)	Diff (%)
Baseline			2,540	-	6.8	-	701	-	55	-	236	-	409	-	7.4	-	35	-	376	-	299	-	602	-	23	-	99	-
Mid-century	2.6	Min [GISS-E2-R]	2,780	10	7.4	9	786	12	62	12	263	12	456	12	8.0	9	39	12	418	11	331	10	661	10	26	12	110	11
		Median	2,900	14	7.2	6	833	19	65	18	279	18	465	14	7.8	6	41	19	437	16	333	11	679	13	27	19	116	17
		Max [HadGEM2-ES]	3,060	21	7.4	9	881	26	70	27	298	26	484	19	8.2	11	45	29	460	22	354	18	718	19	29	26	122	23
	4.5	Min [GISS-E2-R]	2,980	18	8.0	18	850	21	66	19	283	20	491	20	8.8	19	42	20	450	20	357	19	703	17	28	22	117	19
		Median	3,050	20	8.0	17	874	25	68	24	292	24	502	23	8.7	18	43	24	461	22	358	20	712	18	29	24	120	21
		Max [HadGEM2-ES]	3,210	27	7.6	12	932	33	74	33	314	33	512	25	8.3	13	47	35	481	28	370	24	749	24	31	35	128	30
	6.0	Min [NorESM1-M]	2,920	15	7.7	13	834	19	64	17	275	16	487	19	8.4	14	41	17	440	17	342	14	682	13	27	17	114	15
		Median	3,010	19	7.4	9	873	24	68	23	290	23	486	19	8.1	10	43	24	453	20	345	15	700	16	28	23	119	20
		Max [HadGEM2-ES]	3,280	29	7.7	13	957	36	75	36	320	36	520	27	8.4	15	48	39	492	31	375	25	763	27	32	38	131	33
	8.5	Min [BCC-CSM1.1]	3,130	23	7.7	13	912	30	70	28	304	29	499	22	8.4	14	45	29	475	26	357	19	722	20	30	29	124	25
		Median	3,230	27	8.1	18	939	34	73	32	312	32	521	28	8.8	20	46	33	488	30	372	24	747	24	31	33	127	29
		Max [HadGEM2-ES]	3,470	37	8.1	19	1,020	46	80	45	344	46	542	33	8.8	20	51	48	523	39	396	32	806	34	34	48	139	41

[1] RCMs were selected for inclusion in the table based on minimum, median, and maximum total erosion across the whole Wairoa catchment. The median is represented by the mid-point between the middle two RCMs.

[2] 'Wairoa catchment' refers to the whole catchment draining to the coast and includes net sediment contributions from the 'Wairoa corridor' sub-catchment shown in Figures 5–7.

[3] The selected RCMs do not consistently equate to the equivalent min/median/max values for Aniwaniwa and Mōkau due to relative differences in total erosion between RCMs at sub-catchment versus catchment scales. For consistency, we present sediment load results for the selected RCMs across all sub-catchments, which allows comparison between sub-catchments for the same RCM.

[4] Suspended sediment loads reported for the Waiau include net contributions from its sub-catchments (i.e. upper Waiau, lower Waiau, Waihi, Waikaretāheke, Mōkau, Aniwaniwa).

Table 3. Net suspended sediment loads for the whole Wairoa catchment and major sub-catchments under baseline conditions and projected climate change at late century. 'Diff' refers to the percentage difference between the sediment load under climate change compared to the baseline load.

Time period	RCP	Selected RCMs[1]	Wairoa catchment[2]		Aniwaniwa[3]		Hangaroa		Kauhauroa		Mangaaruhe		Mangapoike		Mōkau[3]		Ohinepaka		Ruakituri		Upper Waiau[3]		Waiau[4]		Waihi		Waikaretāheke	
			Load (kt/yr)	Diff (%)	Load (kt/yr)	Diff (%)	Load (kt/yr)	Diff (%)	Load (kt/yr)	Diff (%)	Load (kt/yr)	Diff (%)	Load (kt/yr)	Diff (%)	Load (kt/yr)	Diff (%)	Load (kt/yr)	Diff (%)	Load (kt/yr)	Diff (%)	Load (kt/yr)	Diff (%)	Load (kt/yr)	Diff (%)	Load (kt/yr)	Diff (%)	Load (kt/yr)	Diff (%)
Baseline			2,540	-	6.8	-	701	-	55	-	236	-	409	-	7.4	-	35	-	376	-	299	-	602	-	23	-	99	-
Mid-century	2.6	Min [GISS-E2-R]	2,720	7	7.6	11	765	9	60	8	258	9	445	9	8.2	12	38	9	408	8	334	12	654	9	26	12	108	9
		Median	2,820	11	7.2	5	810	15	64	16	275	16	447	9	7.8	7	41	17	427	13	331	11	667	11	27	17	113	15
		Max [CESM1-CAM5]	3,080	21	7.7	13	891	27	70	27	299	27	499	22	8.3	12	45	28	464	23	355	19	715	19	29	26	121	23
	4.5	Min [GISS-E2-R]	2,960	17	7.7	12	851	21	66	19	283	20	487	19	8.3	13	42	20	445	18	348	16	694	15	28	21	117	18
		Median	3,160	25	7.7	13	922	31	71	29	306	30	515	26	8.4	14	45	31	476	27	360	20	731	21	30	31	125	27
		Max [CESM1-CAM5]	3,430	35	8.2	21	1,010	44	78	41	336	42	551	35	8.7	19	50	43	516	37	393	31	795	32	33	44	137	38
		Min [NorESM1-M]	3,220	27	7.8	14	940	34	72	30	308	31	525	28	8.4	14	46	32	484	29	361	21	735	22	30	31	126	28
	6.0	Median	3,440	36	8.1	19	1,010	44	78	42	336	42	550	34	8.8	19	50	43	517	37	389	30	792	31	33	44	137	39
		Max [HadGEM2-ES]	3,700	46	8.7	27	1,090	56	84	53	361	53	588	44	9.4	28	54	56	553	47	425	42	859	43	36	57	148	49
		Min [GISS-E2-R]	3,760	48	9.0	32	1,110	59	85	55	367	55	607	49	9.8	33	54	57	567	51	429	43	864	43	36	58	149	51
	8.5	Median	4,020	59	8.9	31	1,220	73	92	67	399	69	637	56	9.7	32	59	71	609	62	445	49	913	52	40	71	160	63
		Max [GFDL-CM3]	4,280	69	9.0	32	1,310	86	99	80	429	82	670	64	9.8	33	64	84	649	73	463	55	962	60	42	84	172	74

[1] RCMs were selected for inclusion in the table based on minimum, median, and maximum total erosion across the whole Wairoa catchment. The median is represented by the mid-point between the middle two RCMs.

[2] 'Wairoa catchment' refer to the whole catchment draining to the coast and includes net sediment contributions from the 'Wairoa corridor' sub-catchment shown in Figures 5–7.

[3] The selected RCMs do not consistently equate to the equivalent min/median/max values for Aniwaniwa, Mōkau and upper Waiau due to relative differences in total erosion between RCMs at sub-catchment versus catchment scales. For consistency, we present sediment load results for the selected RCMs across all sub-catchments, which allows comparison between sub-catchments for the same RCM.

[4] Suspended sediment loads reported for the Waiau include net contributions from its sub-catchments (i.e. upper Waiau, lower Waiau, Waihi, Waikaretāheke, Mōkau, Aniwaniwa).

5.3 Model evaluation and limitations

5.3.1 Model evaluation

SedNetNZ is designed to predict spatial patterns in erosion and suspended sediment loads on a mean annual basis for periods spanning multiple decades. It is difficult to quantify model performance over such timescales other than through comparison with measurements of suspended sediment loads (Basher et al. 2018). Often longer-term continuous suspended sediment load data are unavailable. However, discrete measurements of suspended sediment concentration (SSC) and discharge (Q) data may be used to estimate mean annual suspended sediment loads via SSC-Q rating curve methods in combination with longer-term records of river flow (Hicks et al. 2019).

In the Wairoa catchment, an estimate of suspended sediment load based on discharge and suspended sediment concentration data measured between 1968 and1997 and between 1980 and 1996, respectively, is available for a gauging station on the Wairoa River at Marumaru (Hicks et al. 2019). The catchment area upstream of the Wairoa at Marumaru is 1,804 km^2 and covers approximately half of the total Wairoa catchment (3,674 km^2). Using a sediment rating curve approach, Hicks et al. (2019) estimated a mean annual suspended sediment load of 0.92 Mt/yr for this site. The SedNetNZ estimate of suspended sediment load at this location is 1.57 Mt/yr. This difference reflects uncertainties in both the rating curve and SedNetNZ-based estimates of sediment load, as well as differences in land cover between the monitoring period and the model. While SedNetNZ overestimates the load at this site, it represents an improvement on national-scale model estimates, such as the updated Sediment Yield Estimator (SYE), which predicts an uncorrected mean annual suspended sediment load of 3.26 Mt/yr (Hicks et al. 2019).

Previously, Dymond et al. (2016) conducted a sensitivity analysis of model parameters and found uncertainty of approximately ±50% of the total suspended sediment load at the 95% confidence level. The greatest uncertainty arises from the landslide probability density function, landslide sediment delivery ratio (SDR), and gully density.

5.3.2 Model limitations

Erosion process representation

The main limitations in the surficial erosion component of SedNetNZ relate to the calculation of the K and C factors in the NZUSLE. In the present report, the estimate of surficial erosion is based on modelling by Spiekermann et al. (2017) that used a spatially uniform K to represent soil erodibility (equation 1). This could be improved in future model applications by using a spatially variable K based on available soils information (e.g. Neverman, Smith et al. 2021). The C factor represents the effect of vegetation cover on erosion and distinguishes bare ground, pasture, and forest cover. The representation of other land cover types is limited by the availability of data on how different vegetation covers affect surficial erosion rates.

Shallow landslides are initiated by storm events over a triggering threshold. This means the landslide load in any given year can vary significantly from the mean annual landslide load. This inter-annual variability in landslide occurrence is not represented in SedNetNZ. Instead, the storm-triggered shallow landslide contribution to the suspended sediment load is averaged over a multi-decadal timescale. Landslide mapping from historical aerial imagery spanning a 70-year period in the Manawatū catchment (Betts et al. 2017) was used to define the slope thresholds for landslide occurrence and density in the model. Equivalent data were unavailable for the Wairoa catchment.

Both earthflow and gully erosion are represented in SedNetNZ using a spatial averaging approach based on estimated presence and spatial extent of these erosion features in the erosion terrains layer (Dymond et al. 2016). It is therefore possible that earthflow and gully erosion may be represented in sub-catchments that do not contain these features, or may not be represented where they are present. This could be improved through feature-level mapping of gullies and earthflows. This is a very time-consuming process for large catchments. Semi-automated mapping procedures (e.g. Smith et al. 2021) may be developed to capture spatial data on erosion features such as gullies and earthflows, thus providing an alternative approach to manual mapping for representing these features in the model.

Bank erosion modelling requires high-resolution spatial data on channel locations and riparian woody vegetation. Spatial errors in the planform of modelled stream channels and the classification of woody vegetation cover in the riparian zone may be reduced with the forthcoming availability of LiDAR for the Hawke's Bay region. Combining improved channel planform accuracy with a LiDAR-derived canopy height model would enable more accurate delineation of woody vegetation within riparian areas. Improvements in the accuracy of reach sinuosity and channel slope, both inputs to the model, could also be achieved using a more accurate stream network generated from a higher-resolution DEM based on LiDAR.

Climate change projections

There is a high degree of uncertainty in the climate change projections and their impacts, arising from (a) differences between climate models, (b) divergent trajectories of future climate change depending on levels of greenhouse gas emissions, and (c) how these changes affect erosion processes. The choice of climate model affects estimates due to the range of models (RCMs), while the divergence in potential climate futures is captured by the four RCPs and produces a large range in potential impacts. This range means there can be considerable difference between the lowest and highest projections, especially at late century.

Further uncertainty may be introduced related to the applicability of some assumptions for the whole catchment. For example, the adjustment for predicting the change in storm rainfall per 1°C temperature increase (+7.3%) assumes that landslides are triggered by an event with a 48-hour duration and an average recurrence interval (ARI) of 30 years. A uniform triggering threshold of 150 mm in 48 hours has been used to estimate landslide density, but this threshold may vary for different terrains and different mass movement processes (e.g. Reid & Page 2003; Basher et al. 2020).

There is also a lack of information on the relationship between climate change and erosion processes in New Zealand. Basher et al. (2020) identified this knowledge gap, noting there had been only a few studies in New Zealand on the potential impacts of climate change on erosion, and most of these consisted of general statements about likely trends rather than quantifying change. For instance, Crozier (2010) reviewed the basis for assessing the impact of climate change on landslides and found that although there is a strong theoretical basis for increased landslide activity in response to predicted climate change, there is a high level of uncertainty resulting from the error margins inherent in downscaling GCMs spatially and temporally. Due to the high uncertainty, the results of the climate change projections should, therefore, be interpreted as indicative of trends rather than absolute values (Basher et al. 2020).

6 Conclusions

Suspended sediment loads across the Wairoa catchment are likely to increase in the future under climate change. The modelled mean annual suspended sediment load delivered to the coast under recent baseline conditions is 2.5 Mt/yr. Under future climate scenarios the range in end-of-catchment suspended sediment loads is estimated at 2.8–3.5 Mt/yr and 2.7–4.3 Mt/yr by mid- and late century, respectively. These changes correspond to increases of 10–37% and 7–69% compared to the baseline sediment load by mid- and late century, respectively.

Further modelling work is planned within the Whitiwhiti Ora project to examine how different land-use scenarios affect suspended sediment loads under climate change. The scenarios will be developed in partnership with the Wairoa Tripartite. SedNetNZ will be used to quantify the combined impacts of land use and climate change on suspended sediment loads in the catchment. This information will inform related work linking river sediment and its impacts on mahinga kai species and sites of cultural significance.

7 Acknowledgements

This work was funded by the New Zealand Ministry of Business, Innovation and Employment's Our Land and Water National Science Challenge (Toitū te Whenua, Toiora te Wai), contract C10X1901, as part of the Whitiwhiti Ora (WWO) – Land Use Opportunities programme. We acknowledge NIWA for providing modelled mean annual flood statistics for use in the WWO programme.

8 References

Abernethy B, Rutherfurd ID 2000. The effect of riparian tree roots on the mass-stability of riverbanks. Earth Surface Processes and Landforms 25(9): 921–937.

Arulanandan K, Gillogley E, Tully R 1980. Development of a quantitative method to predict critical shear stress and rate of erosion of natural undisturbed cohesive soils. USACE, Waterways Experiment Station Technical Report GL-80-5. Vicksburg, MS, USACE.

Basher L, Spiekermann R, Dymond J, Herzig A, Ausseil A-G 2018. SedNetNZ, SLUI and contaminant generation. Part1: Sediment and water clarity. Manaaki Whenua – Landcare Research contract report LC3135 prepared for Horizons Regional Council.

Basher L, Spiekermann R, Dymond J, Herzig A, Hayman E, Ausseil A-G 2020. Modelling the effect of land management interventions and climate change on sediment loads in the Manawatū–Whanganui region. New Zealand Journal of Marine and Freshwater Research 54(3): 490–511.

Betts H, Basher L, Dymond J, Herzig A, Marden M, Phillips C 2017. Development of a landslide component for a sediment budget model. Environmental Modelling & Software 92: 28–39.

Brune GM 1953. Trap efficiency of reservoirs. Eos, Transactions American Geophysical Union 34(3): 407–418.

Collins D, Montgomery K, Zammit C 2018. Hydrological projections for New Zealand rivers under climate change. NIWA Contract Report No. 2018193CH prepared for the Ministry for the Environment.

Crosato A 2009. Physical explanations of variations in river meander migration rates from model comparison. Earth Surface Processes and Landforms 34: 2078–2086.

Crozier MJ 2010. Deciphering the effect of climate change on landslide activity: a review. Geomorphology 124(3): 260–267.

De Rose RC 2013. Slope control on the frequency distribution of shallow landslides and associated soil properties, North Island, New Zealand. Earth Surface Processes and Landforms 38(4): 356–371.

De Rose RC, Basher LR 2011. Strategy for the development of a New Zealand SedNet. Landcare Research Contract Report LC226 for AgResearch and Ministry of Science and Innovation Landcare Research Contract Report LC226 for AgResearch and Ministry of Science and Innovation.

De Rose RC, Prosser IP, Weisse M, Hughes AO 2003. Patterns of erosion and sediment and nutrient transport in the Murray-Darling Basin. CSIRO Land and Water Technical Report 32/03.

Douglas GB, Trustrum NA, Brown IC 1986. Effect of soil slip erosion on Wairoa hill pasture production and composition. New Zealand Journal of Agricultural Research 29: 183–192.

Dunn IS 1959. Tractive resistance of cohesive channels. Journal of the Soil Mechanics and Foundations Division 85(3): 1–24.

Dymond J, Herzig A, Basher L, Betts HD, Marden M, Phillips CJ, Ausseil A-GE, Palmer DJ, Clark M, Roygard J 2016. Development of a New Zealand SedNet model for assessment of catchment-wide soil-conservation works. Geomorphology 257: 85–93.

Dymond JR, Betts HD, Schierlitz CS 2010. An erosion model for evaluating regional land-use scenarios. Journal of Environmental Modelling Software 25(3): 289–298.

Dymond JR, Jessen MR, Lovell LR 1999. Computer simulation of shallow landsliding in New Zealand hill country. International Journal of Applied Earth Observation and Geoinformation 1(2): 122–131.

Dymond JR, Shepherd JD 2004. The spatial distribution of indigenous forest and its composition in the Wellington region, New Zealand, from ETM+ satellite imagery. Remote Sensing of Environment 90: 116–125.

Elliott AH, Semadeni-Davies AF, Shankar U, Zeldis JR, Wheeler DM, Plew DR, Rys GJ, Harris SR 2016. A national-scale GIS-based system for modelling impacts of land use on water quality. Environmental Modelling & Software 86: 131–144.

Eyles GO 1983. The distribution and severity of present soil erosion in New Zealand. New Zealand Geographer 39: 12–28.

Fryirs KA, Wheaton JM, Brierley GJ 2016. An approach for measuring confinement and assessing the influence of valley setting on river forms and processes. Earth Surface Processes & Landforms 41: 701–710.

Gill MA 1979. Sedimentation and useful life of reservoirs. Journal of Hydrology 44(1): 89–95.

Guy GG 1977. Landslide investigations, Main North Line Railway, South Island, New Zealand. Unpublished thesis, University of Canterbury. http://ir.canterbury.ac.nz/handle/10092/8095.

Hall JE, Holzer DM, Beechie TJ 2007. Predicting river floodplain and lateral channel migration for salmon habitat conservation 1. Journal of the American Water Resources Association 43(3): 786–797.

Hanson GJ, Simon A 2001. Erodibility of cohesive streambeds in the loess area of the midwestern USA. Hydrological Processes 15(1): 23–38.

Hickin EJ, Nanson GC 1984. Lateral migration rates of river bends. Journal of Hydraulic Engineering 110(11): 1557–1567.

Hicks DM, Semadeni-Davies A, Haddadchi A, Shankar U, Plew D 2019. Updated sediment load estimator for New Zealand NIWA Client Report No: 2018341CH.

Hubble TCT, Docker BB, Rutherfurd ID 2010. The role of riparian trees in maintaining riverbank stability: a review of Australian experience and practice. Ecological Engineering 36(3): 292–304.

IPCC 2013. Climate change 2013: the physical science basis. Contribution of Working Group I to the Fifth Assessment Report of the Intergovernmental Panel on Climate Change. Cambridge, UK, and New York, NY, Cambridge University Press. 1535, doi:10.1017/CBO9781107415324. p.

Julian JP, Torres R 2006. Hydraulic erosion of cohesive riverbanks. Geomorphology 76(1): 193–206.

Konsoer KM, Rhoads BL, Langendoen EJ, Best JL, Ursic ME, Abad JD, Garcia MH 2016. Spatial variability in bank resistance to erosion on a large meandering, mixed bedrock-alluvial river. Geomorphology 252: 80–97.

Manderson A, Dymond JR, Ausseil A-G 2015. Climate change impacts on water quality outcomes from the Sustainable Land Use Initiative (SLUI). Horizons Report No. 2015/EXT/1451.

Marden M, Herzig A, Basher L 2014. Erosion process contribution to sediment yield before and after the establishment of exotic forest: Waipaoa catchment, New Zealand. Geomorphology 226: 162–174.

Marden M, Phillips CJ, Rowan D 2008. Recurrent displacement of a forested earthflow and implications for forest management, East Coast Region, New Zealand. IAHS publication 325: 491–501.

Ministry for the Environment 2018. Climate change projections for New Zealand atmospheric projections based on simulations undertaken for the IPCC 5th Assessment. 2nd edn. Wellington, Ministry for the Environment.

Neverman A, Donovan M, Smith HG, Ausseil A-G, Zammit C 2021. National-scale erosion and catchment sediment loads under projected climate change – a summary of model outputs Manaaki Whenua – Landcare Research Contract Report LC4066 for OLW.

Neverman A, Smith HG 2022. SedNetNZ modelling for freshwater planning in Otago. Manaaki Whenua – Landcare Research Contract Report LC5016 prepared for Otago Regional Council.

Neverman A, Smith HG, Herzig A, Basher LR 2021. Modelling baseline suspended sediment loads and load reductions required to achieve Draft Freshwater Objectives for Southland. Manaaki Whenua – Landcare Research Contract Report LC3749 prepared for Environment Southland.

Newsome PFJ, Wilde RH, Willoughby EJ 2008. Land resource information system spatial data layers: data dictionary. Palmerston North, NZ, Landcare Research. http://digitallibrary.landcareresearch.co.nz/cdm/ref/collection/p20022coll14/id/67.

NIWA 2021. CliFlo: NIWA's National Climate Database on the Web. cliflo.niwa.co.nz.

Page MJ, Trustrum NA, Dymond JR 1994. Sediment budget to assess the geomorphic effect of a cyclonic storm, New Zealand. Geomorphology 9(3): 169–188.

Palmer D, Dymond J, Basher L, Ausseil A-G, Herzig A, Betts H, Spiekermann R 2017. SedNetNZ modelling to evaluate and quantify sediment sources from the Tukituki catchment, Hawke's Bay. Manaaki Whenua – Landcare Research Contract Report LC1991 prepared for Hawke's Bay Regional Council.

Palmer D, Dymond J, Mueller M, Herzig A, Spiekermann R, Basher L 2016. SedNetNZ modelling to estimate sediment sources from the TANK, South Coast, and Porangahau watersheds. Manaaki Whenua – Landcare Research Contract Report LC2599 prepared for Hawke's Bay Regional Council.

Polvi LE, Wohl E, Merritt DM 2014. Modeling the functional influence of vegetation type on streambank cohesion. Earth Surface Processes and Landforms 39(9): 1245–1258.

Reid LM, Page MJ 2003. Magnitude and frequency of landsliding in a large New Zealand catchment. Geomorphology 49(1-2): 71–88.

Sibson R 1981. A brief description of natural neighbor interpolation. In: Barnett V ed. Interpolating multivariate data. Chichester, UK, John Wiley. Pp. 21–36.

Simon A, Collison AJC 2002. Quantifying the mechanical and hydrologic effects of riparian vegetation on streambank stability. Earth Surface Processes and Landforms 27(5): 527–546.

Smith HG, Spiekermann R, Betts H, Neverman AJ 2020. Application of a revised bank erosion model to update SedNetNZ results for Hawke's Bay. Manaaki Whenua – Landcare Research Contract Report LC3740 prepared for Hawke's Bay Regional Council.

Smith HG, Spiekermann R, Betts H, Neverman AJ 2021. Comparing methods of landslide data acquisition and susceptibility modelling: examples from New Zealand. Geomorphology 381: 107660.

Smith HG, Spiekermann R, Dymond J, Basher L 2019. Predicting spatial patterns in riverbank erosion for catchment sediment budgets. New Zealand Journal of Marine and Freshwater Research 53(3): 338–362.

Sood A 2014. Improved bias corrected and downscaled regional climate model data for climate impact studies: validation and assessment for New Zealand. Retrieved from www.researchgate.net/publication/265510643_Improved_Bias_Corrected_and_Downscaled_Regional_Climate_Model_Data_for_Climate_Impact_Studies_Validation_and_Assessment_for_New_Zealand

Spiekermann R, Betts H, Dymond J, Basher L 2017. Volumetric measurement of river bank erosion from sequential historical aerial photography. Geomorphology 296: 193–208.

Thorne CR 1990. Effects of vegetation on riverbank erosion and stability. In: Thornes JB ed. Vegetation and erosion. Chichester, UK, John Wiley & Sons. Pp. 125–144.

Trustrum NA, Gomez B, Page MJ, Reid LM, Hicks DM 1999. Sediment production, storage and output: the relative role of large magnitude events in steepland catchments. Zeitschrift für Geomorphologie N.F. Supplement 115: 71–86.

Vale SS, Smith HG, Neverman A, Herzig A 2021. Application of SedNetNZ with land management and climate change scenarios and temporal disaggregation in the Bay of Plenty Region. Manaaki Whenua – Landcare Research Contract Report LC4002 prepared for Bay of Plenty Regional Council.

Woods R, Hendrikx J, Henderson R, Tait A 2006. Estimating mean flow of New Zealand rivers. Journal of Hydrology (New Zealand) 45(2): 95–109.

Wynn T, Mostaghimi S 2006. The effects of vegetation and soil type on streambank erosion, Southwestern Virginia, usa1. Journal of the American Water Resources Association 42(1): 69–82.

Zhang X, Phillips C, Pearce A 1991. Surface movement in an earthflow complex, Raukumara Peninsula, New Zealand. Geomorphology 4(3): 261–272.